Comparison of Magnetic and Electromagnetic Anomalies Caused by Underground Structures

I.J. Won and Dean Keiswetter
Geophex, Ltd.
Raliegh, North Carolina

ABSTRACT

Magnetic and electromagnetic (EM) methods are perhaps the most convenient and popular geophysical survey methods for detecting buried manmade objects, which is due to their non-intrusiveness, light field logistics, high survey speed, and the quality of information. One should always consider the two methods as the precursor to any geophysical survey. Often, the data resulting from the two methods are sufficient for characterizing buried objects.

In this paper, we present magnetic and EM data collected at four sites: (1) Cloud Chamber at the Nevada Test Site, (2) Anacostia Metro Tunnels in Washington, D.C., (3) Cold Test Pit at Idaho National Engineering Laboratory, and (4) Unexploded ordnance site at Jefferson Proving Ground, Indiana. The first two sites may be considered typical underground facilities. The last two sites, however, contain small buried objects (storage tanks, ordnance, etc.) specifically prepared to test various geophysical methods for detection and, possibly, discrimination.

We find through these and numerous other comparisons that broadband EM data are superior to magnetic data in terms of the amount and the quality of information. The monopolar EM anomaly is invariably easier to interpret, and thus can locate a buried target more accurately than the dipolar magnetic anomaly. In addition, the EM method senses both electrically conductive and magnetically permeable targets. In contrast, the magnetic method responds only to permeable, or ferrous, metals. In that sense, the magnetic method should be considered a subset of the EM method, or a special "passive" EM method at zero frequency.

Introduction

From the viewpoints of non-intrusiveness, field logistics, and survey speed, the magnetic and electromagnetic (EM) methods stand far ahead of other geophysical techniques, including gravity, electrical resistivity, seismic refraction or reflection, and ground-probing radar (GPR).

Intrusiveness: Magnetic and EM sensors are commonly man-portable. The methods do not require ground contact (e.g., seismic and electrical resistivity) or demand a stabilized survey platform (e.g., gravity). The GPR is sensitive to ground roughness, particularly at high frequencies.

Field Logistics: Portable magnetic and EM sensors are usually light in weight, simple to operate, and consume relatively little electrical power. The methods do not involve an array of sensors connected by tangled cables and wires, as would be common for seismic, electrical resistivity, and GPR methods.

Survey Speed: Magnetic and EM sensors can operate continuously in time and in motion. With high-capacity data-logging electronics common to modern portable sets, the sensors can collect over tens of thousand survey points per hour. For a typical high-resolution survey, this translates to an areal coverage of one acre (0.4 hectare) or more per hour. The data can be downloaded to a portable computer and the survey results can be viewed, typically in a color contour format, on site within a few minutes.

Based on these advantages, one should always consider conducting magnetic and EM surveys as the precursor to any ground geophysical surveys for detecting buried objects, including underground facilities. If nothing else, they are quick and easy and provide a first geophysical view of the site. Quite often, the two methods provide enough data to proceed with planned site activities.

Most manmade objects, except for plastics, contain metals that are easy to detect by the magnetic and/or EM method. Quite often, the two methods can be complementary. In this article, we compare the viability of the two methods and present example data collected over known buried objects. We limit our discussions in this article to ground-level geophysical surveys, although similar arguments can be made for airborne geophysical surveys.

Nature of Magnetic Anomalies

Whether induced or permanent, a buried, ferrous object exhibits basically a dipolar magnetic source. Any object may be represented as a sum of magnetic dipoles having various magnetic moments and dipole orientations. The surface manifestation of this source on a survey plane (i.e., the ground) can be varied according to the source distribution, topography, and geomagnetic latitude.

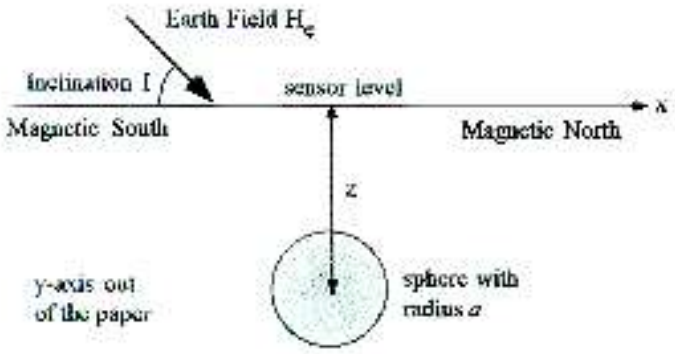

Figure 1. Geometry of a permeable sphere placed in the earth magnetic field.

As a heuristic example of a unit magnetic source, consider a permeable sphere placed in the earth magnetic field as shown fig. 1. The induced magnetic anomaly ΔH(in nT) can be shown as

$$\Delta H = \frac{kVH_e \sin I}{(x^2+y^2+z^2)^{5/2}}\left\{\sin I\left[(x^2+y^2-2z^2)-3xz\cot I\right]\right.$$

$$\left.+\cos I\left[(-2x^2+y^2+z^2)\cot I-3xz\right]\right\} \qquad (1)$$

where

k: magnetic susceptibility (emu) of the sphere,
V: volume of the sphere,
H_e: magnitude of the earth field in nT,
I: local geomagnetic inclination, and
(x, y, z): sensor location with respect to the sphere.

Figure 2 shows the computed magnetic anomaly for a sphere having a radius of 25 cm placed in a free space. The anomaly is computed at geomagnetic latitude of 45° with an earth field of 46,000 nT. The depth of the sphere is one meter (top), two meters (middle), and three meters (bottom). A solid circle at the center of each map indicates the sphere location, as well as its relative size.

The example shows the dipolar nature of the measured magnetic anomaly; the source object is situated somewhere along the steep magnetic gradient connecting the positive and negative anomalies. This can be a serious drawback of the magnetic method: the source is located on the magnetic slope rather than the peaks, which renders intuitive interpretation difficult. Many geophysical methods work well as "bump finders" to locate a target. In magnetics, however, one must find a combination of positive and negative bumps and locate a target somewhere in between.

Nature of Electromagnetic Anomalies

Unlike the magnetic method in which one measures an existing field at a point, the active EM method brings in many more measurement variables. We limit this discussion to active EM systems that have a fixed transmitter-receiver (T-R) geometry so compact as to be man-portable. All EM data shown here were acquired using the GEM-2 (Won et al., 1996) or GEM-3 (Won et al., 1997) sensors developed by Geophex. For such portable EM sensors, the T-R separation is usually much smaller than the distance to the target, resulting in an essentially co-located, or monostatic, system. Most common metal detectors have monostatic geometry.

Figure 3 shows the basic geometry of an active EM system involving a transmitter and a receiver coil. As a heuristic example, consider a sphere having an infinite electrical conductivity located at (x, y, z) as indicated in fig. 3. For this limiting case, the response is only in the inphase component with no quadrature component. The ratio h(x) of the secondary field from the sphere to the primary transmitter field at the receiver coil can be shown as:

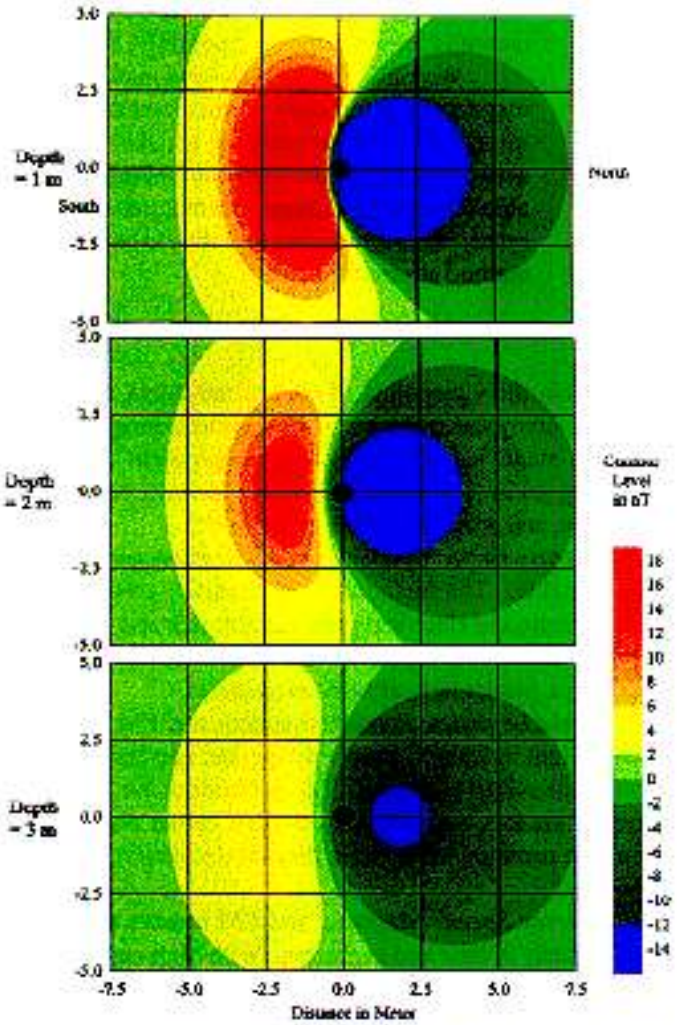

Figure 2. Computed magnetic anomaly for a permeable sphere placed in a free space. The sphere is assumed to have a radius of 25 cm and is located at three different depths of 1-m (top), 2-m (middle), and 3-m (bottom).

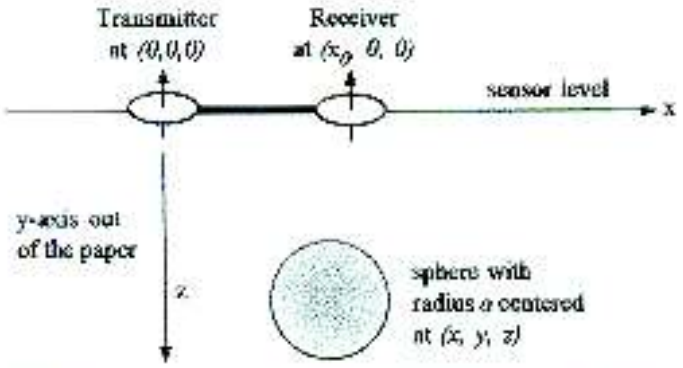

Figure 3. Geometry of an active EM system involving a transmitter and a receiver loop.

$$h(x)=\frac{3V\chi_0^3}{8\pi}\frac{9z^2(xx_0-x^2-y^2)+(2z^2-x^2-y^2)[2z^2-(x_0-x)^2-y^2]}{(x^2+y^2+z^2)^{5/2}[(x_0-x)^2+y^2+z^2]^{5/2}} \quad (2)$$

where V is the sphere volume and x_0 is the distance between the two coils as shown in fig. 3. For the GEM-2 sensor (having a T-R separation of about 1.6 m), we have two receiver coils (in line with the transmitter coil) that are designed to null the primary field in free space. Therefore, the signal output combined by the two receiver coils constitutes the anomaly. Often, we use a part-per-million (ppm) unit defined as:

$$ppm\ \frac{secondary\ magnetic\ field\ at\ receiver\ coil}{Primary\ magnetic\ field\ at\ receiver\ coil} \quad (3)$$

The ppm unit (commonly a complex number made of the inphase and quadrature components) is dependent on the sensor geometry and has little physical significance. However, it is a convenient means of normalizing the anomaly strength against the transmitter strength. Data expressed in a ppm unit is sufficient for detecting and characterizing isolated anomalies.

Figure 4 shows the computed GEM-2 anomaly over a perfectly conducting sphere. The sphere is assumed to have a radius of 25 cm and is located at three different depths of one meter (top), two meters (middle), and three meters (bottom). Figure 4 indicates that when the target depth is shallower than the T-R separation, we notice a slight elongation along the T-R axis (top). As the target depth increases, the anomaly becomes circular (bottom). Unlike the source location for a magnetic anomaly, the target sphere is always situated at the center of the EM anomaly. This coincidence of the target and the anomaly peak, an important feature of monostatic or near-monostatic EM sensors (e.g., GEM-2 and GEM-3), renders data interpretation simple and intrinsic.

Additional advantages of the EM method come from the fact that it senses both electrically conductive and magnetically permeable targets. In contrast, the magnetic method responds only to permeable, or ferrous, metals. In that sense, the magnetic method may be considered a subset of the EM method, or it is a special "passive" EM method at zero frequency.

While conductive targets manifest a strong positive inphase anomaly, permeable targets produce a strong negative inphase anomaly, particularly at low frequencies. For a rigorous treatment of this subject, one should consider a finitely conductive and permeable sphere excited by a dipole EM source. This is one of the most classical geophysical problems with a known analytic solution (Wait, 1953). This discussion is out of the scope of this article. One of the interesting features is that when the sphere is ferrous, the EM anomaly exhibits a large negative inphase component at low frequencies and, at zero frequency, shows a DC magnetic response. At a very low frequency, a ferrous sphere is magnetized along

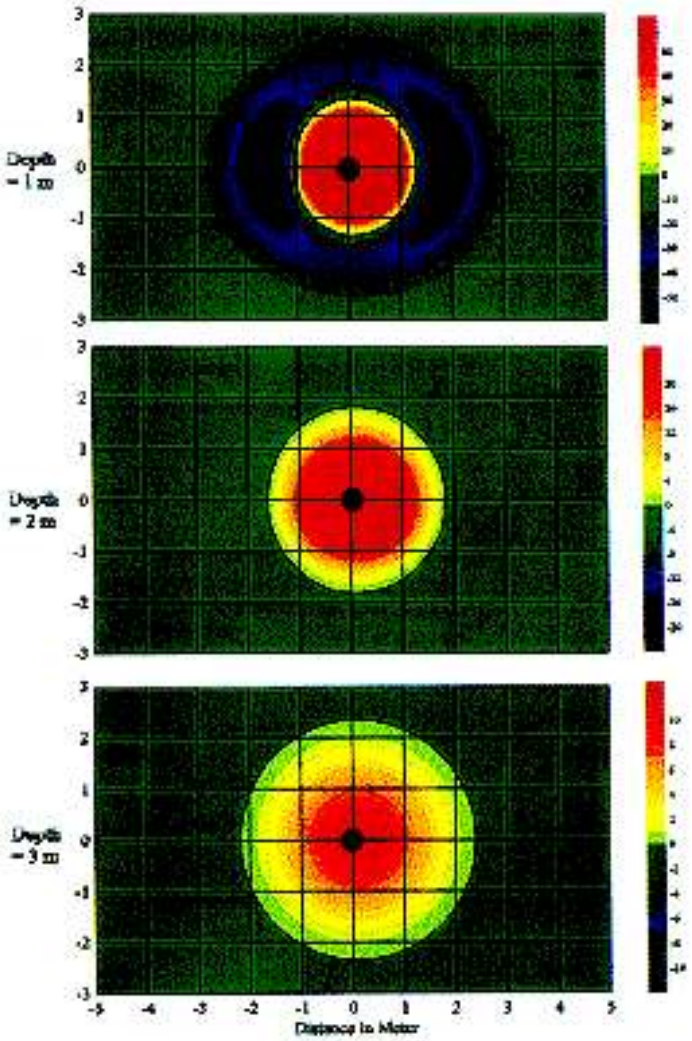

Figure 4. Computed GEM-2 anomaly over a perfectly conducting sphere. The sphere is assumed to have a radius of 25 cm and is located at three different depths of 1-m (top), 2-m (middle), and 3-m (bottom).

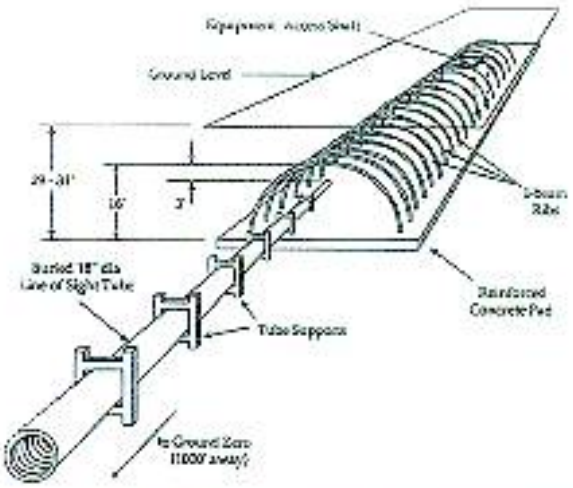

Figure 5. Sketch of the underground Cloud Chamber at the NTS.

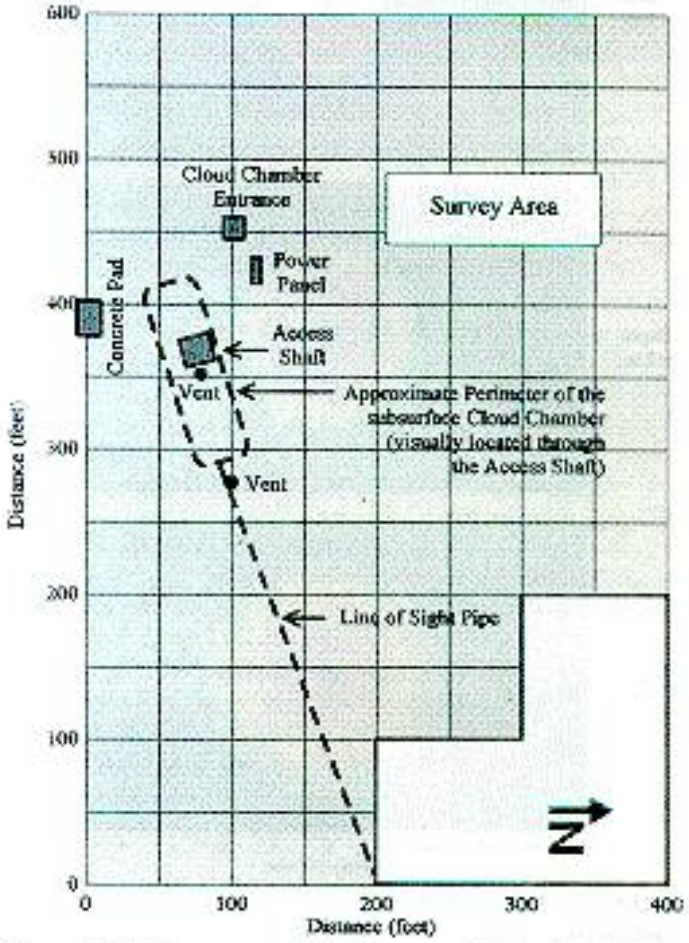

Figure 6. Major exposed features and survey coverage at the Cloud Chamber site.

the external field lines which, in this case, are generated by a magnetic dipole transmitter. As the frequency increases, the inphase component becomes dominantly positive with a vanishing quadrature component.

Such phase relationship of the broadband EM anomaly can be exploited not only for detecting a target but for discriminating it in terms of target's material composition. If we can measure a target's EM response in a truly broadband, we may be able to identify the target as a particular known object based upon its spectral signature.

Field Examples

In the following, we present magnetic and EM data collected at four sites: (1) Cloud Chamber at the Nevada Test Site, (2) Anacostia Subway Tunnels in Washington, D.C., (3) Cold Test Pit at Idaho National Engineering Laboratory, and (4) Unexploded Ordnance at Jefferson Proving Ground. The first two sites may be considered typical underground facilities. The last two sites, however, contain small, buried objects (storage tanks, ordnance shells, etc.) specifically prepared to test various geophysical methods for detection and, possibly, discrimination. We included the last two examples mainly because small, isolated targets manifest simple anomalies that are easy to visualize, interpret, and compare.

Cloud Chamber at the Nevada Test Site

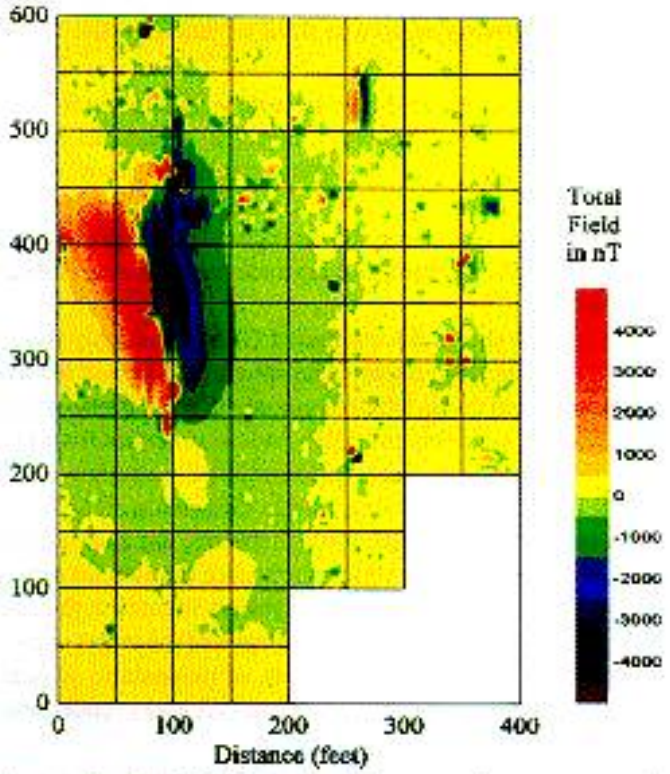

Figure 7. Total-field magnetic anomaly map over the Cloud Chamber.

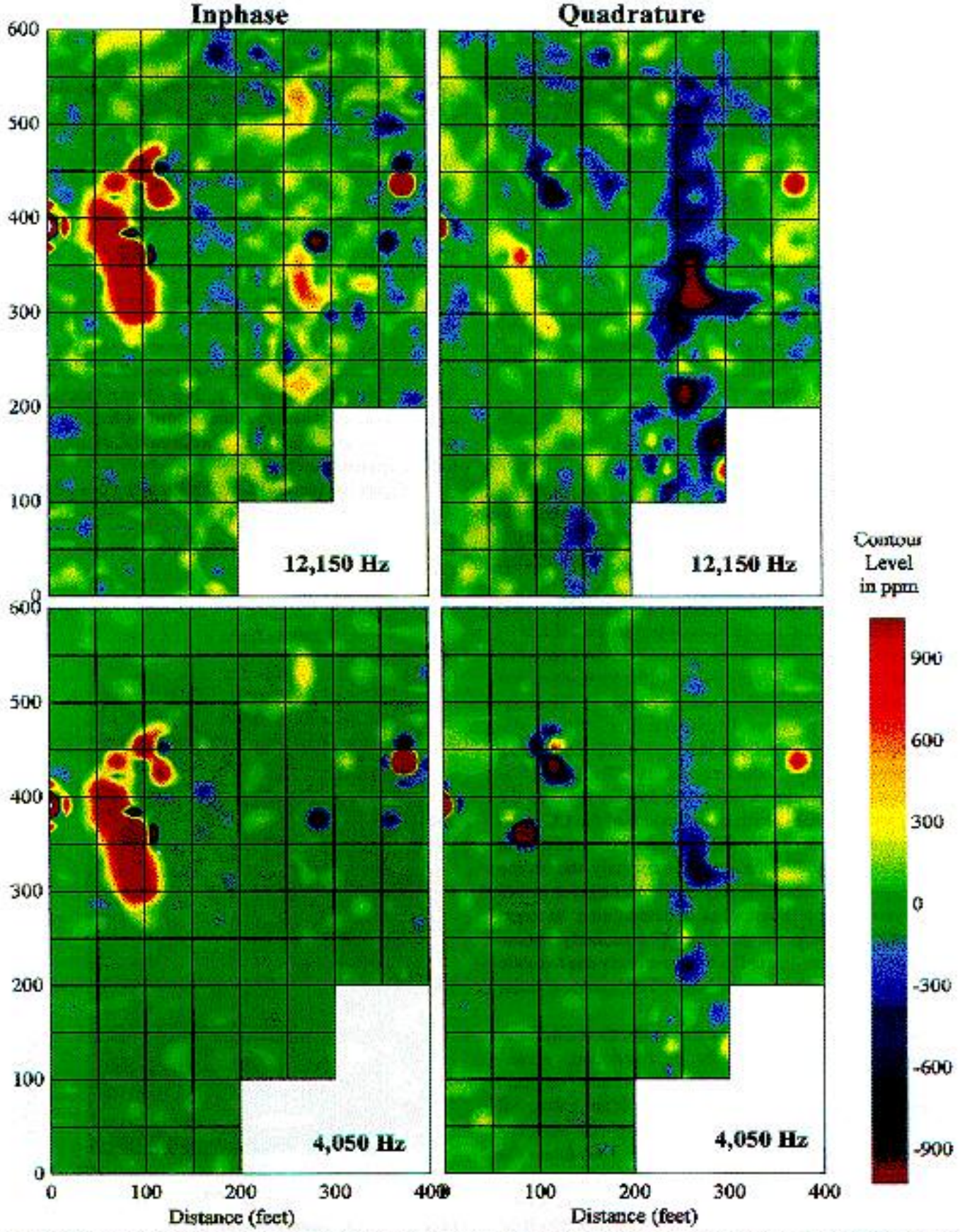

Figure 8. EM anomaly maps from GEM-2 data at two frequencies of 12,150 Hz and 4,050 Hz. The GEM-2 was used in a vertical-dipole mode.

The Cloud Chamber (CC) was built in 1960s in Yucca Flat as a part of an experimental facility associated with underground nuclear tests. Figure 5 shows the structure that is buried in an alluvial basin. The CC is 140-ft long and 32-ft wide at its base and 16-ft high along the center (Cogbill, 1995). Presently, the CC is partially exposed with its equipment access shaft and an entrance stairwell as shown approximately in fig. 6.

Figure 7 shows a total-field magnetic anomaly map prepared from the data obtained by Cogbill (1995) who used a cesium-vapor magnetometer (Geometrics 822L) to collect over 150,000 data points along north-south lines spaced at 5-ft intervals. The CC exhibits a predominantly dipolar magnetic anomaly having a peak-to-peak amplitude of more than 10,000 nT. When compared with fig. 6, we note that the central CC axis runs almost along the line dividing the positive (south) and negative (north) magnetic anomalies.

It is not surprising that the magnetic data did not indicate the presence of the "line-of-sight" tube (see fig. 5) that has a diameter of 18 inches and is buried at about 25 feet in depth. The tube is made of stainless steel (nonmagnetic). Many small anomalies can be correlated with exposed features as indicated in fig. 6. Small anomalies away from the CC are caused by a plethora of metallic debris (e.g., tubes, cables, sheet metals) strewn over the surface.

Figure 8 shows four EM anomaly maps, from the same area, from GEM-2 data at two (arbitrary) frequencies of 12,150 Hz and 4,050 Hz. For this survey, the GEM-2 was used in a "horizontal" mode in which the plane of the transmitter and receiver coils is horizontal (thus, vertical dipoles). The contour levels are in the ppm unit discussed earlier.

Being a largely metallic structure, the CC manifests a strong inphase anomaly at both frequencies. All exposed features are also well correlated. When we overlay fig. 6 on the EM maps, we note that the structural extent of the CC coincides very well with the positive EM anomaly (the red area in the inphase maps). Unlike the magnetic anomaly, the outline of the EM anomaly, therefore, represents the target structure itself; this greatly simplifies the task of determining the target location with respect to the measured EM anomaly. Some linear quadrature anomalies in fig. fig. 8 are likely due to subtle changes in ground conductivity resulting from geologic variation or previous excavation activities.

It was disappointing that the EM maps shown in fig. 8 failed to detect the line-of-sight tube. As a variation, we conducted an additional survey using the GEM-2 in a "vertical" mode in which the plane of all coils is vertical (thus, horizontal dipoles). We also aligned the T-R axis along east-west, approximately parallel with the tube (see fig. 6). The rationale is that this configuration should provide twice stronger coupling between the GEM-2 and the tube. Figure 9 shows the additional GEM-2 data at 7,290 Hz, collected over a 200-ft by 300-ft area above the line-of-sight tube. For easy comparison, the x-y coordinates are the same with figs. 6, 7, and 8. The tube is clearly seen in this data at this frequency. Indications of the tube in the quadrature data are weak at several (arbitrary) frequencies used for this survey. Apparently, the GEM-2 is the only geophysical sensor that has detected this line-of-sight tube.

Anacostia Metro Tunnels in Washington, D.C.

We conducted a combined magnetic and EM survey near Anacostia Metro Station (Green Line) in Washington, D.C. The magnetic survey employed two vertically separated, cesium-vapor sensors (Geometrics Model G-858). The GEM-2 employed two frequencies, 9,030 Hz and 2,010 Hz, at this site. All survey lines were spaced at 5-ft intervals; along the line, the data density is about one per foot.

Figure 10 (top row) shows the total-field magnetic and the vertical magnetic gradient maps over a 200-ft by 200-ft area directly above the tunnel pair. It is known that the tubes at this location, each having a diameter of 14 feet, are buried at a depth of about 40 feet. The horizontal distance of the two tubes is approximately 40 ft.

Figure 10 (second and third rows) shows the GEM-2

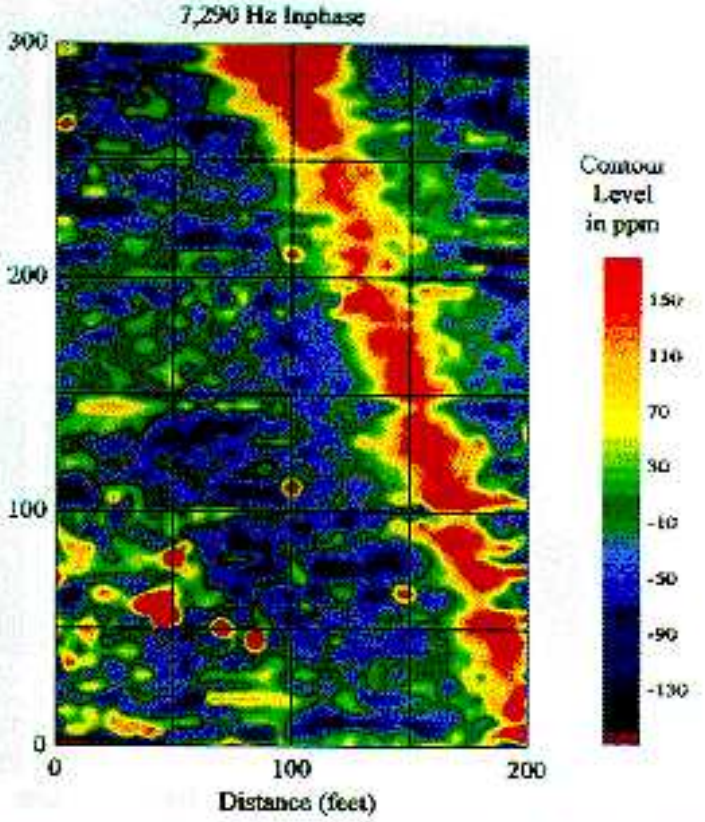

Figure 9. EM anomaly map at 7,290 Hz collected above the line-of-sight tube. The GEM-2 was used in a horizontal-dipole mode.

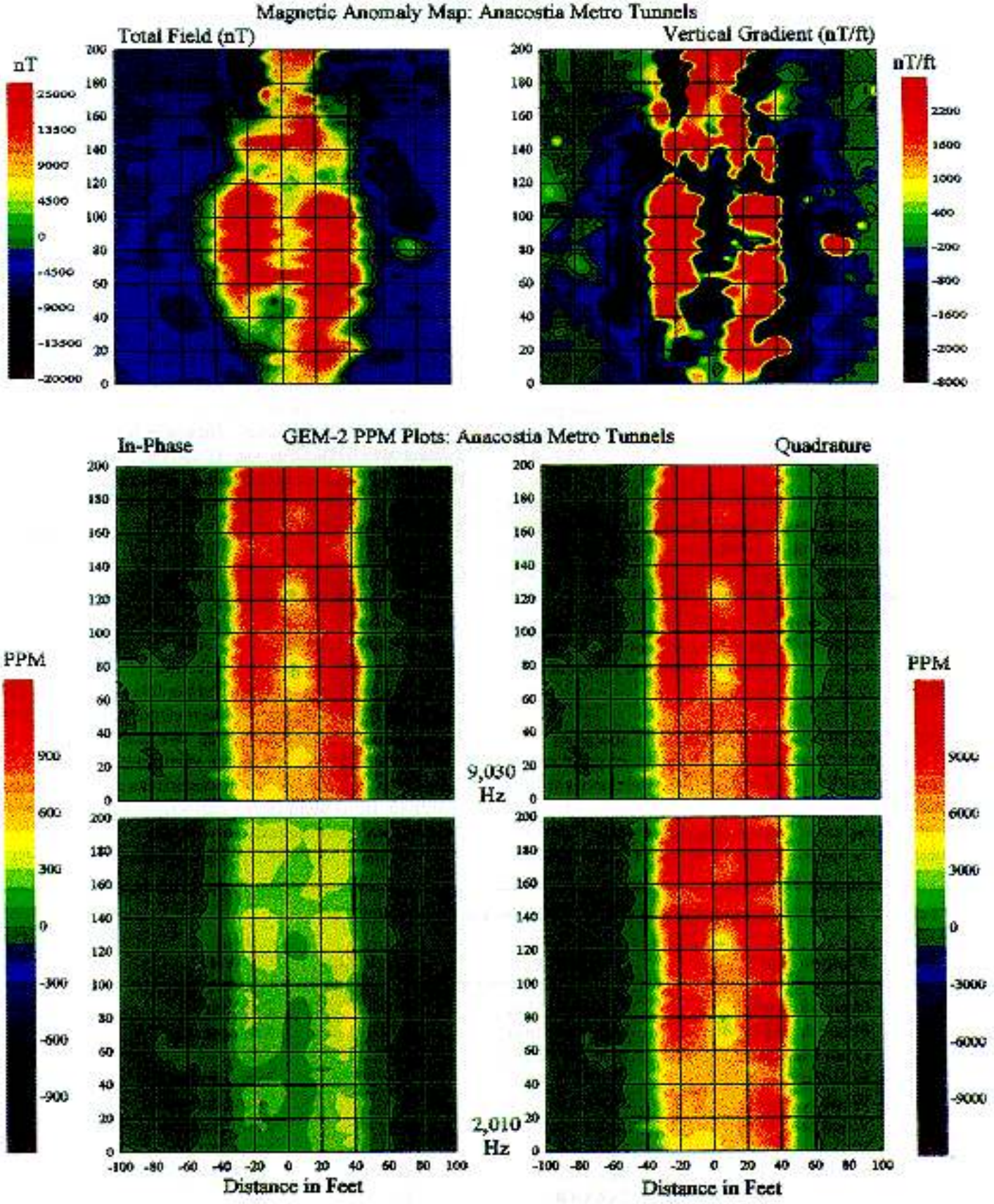

Figure 10. Total-field magnetic, vertical magnetic gradient, and EM anomaly maps (at 9,030 Hz and 2,010 Hz) directly over a 200-ft by 200-ft area directly above the Anacostia tunnel pair.

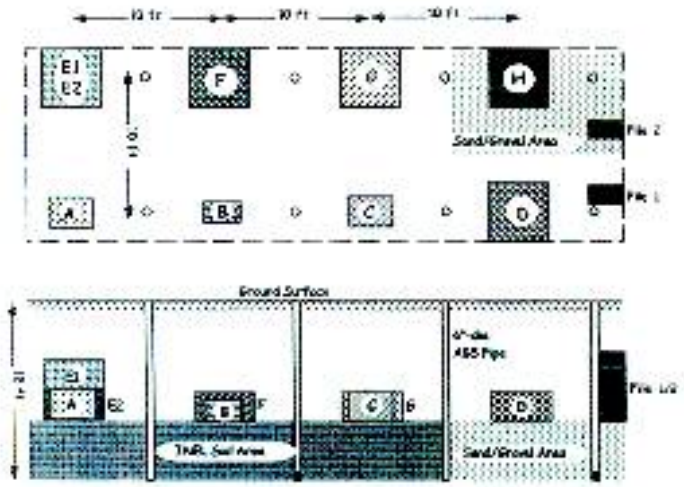

Figure 11.Ten separate waste forms buried in the Calibration Cells of the Cold Test Pit, INEL. The site has dimensions of about 40 by 13 ft. To insure the proper coverage, the geophysical survey grid extended over a 60-ft by 30-ft area.

data over the same area. All GEM-2 data shown below were collected in a vertical mode. The EM data indicates the presence of the two tubes much more clearly than does the magnetic data. The magnetic map at this site is somewhat puzzling in a sense that it lacks the strong linearity manifested by the EM data. It is interesting to note that the EM data strongly suggests that the tubes are regularly disjointed at approximately 50-ft intervals; the tubes are made and joined at 50-ft sections.

Cold Test Pit at Idaho National Engineering Laboratory

Under the Environmental Restoration Program of the U.S. Department of Energy, the U.S. Geological Survey in Denver conducted a program to test modern EM sensors for their ability in mapping and characterizing buried waste. The demonstration site is known as the Cold Test Pit (CTP) at the Idaho National Engineering Laboratory. Under this invitation, Geophex conducted both magnetic and GEM-2 surveys at CTP. We present in this paper a small portion of the dataset collected over the Calibration Cells site.

The local geology consists of surficial clayey soil underlain by thick basalt flows. Figure 11 shows the ten separate waste forms buried in the Calibration Cells. Table 1 lists details of the waste forms. The site has dimensions of about 40 by 13 ft. To insure the proper coverage, however, the USGS established a survey grid over a 60 by 30-ft area centered at the site.

We collected magnetic data using a Geometrics G858 cesium-vapor magnetometer with two sensing heads vertically separated by 30 inches. The magnetic data were collected along east-west lines at a 2-ft line spacing and about 0.75-ft data interval along each line. Figure 12 (top row) shows the total field and the vertical gradient maps.

The GEM-2 survey over the site was conducted employing a similar data density. The rest of fig. 12 shows GEM-2 data at three frequencies, viz., 12,150 Hz, 7,200 Hz, and 2,040 Hz. GEM-2 data were collected in a "vertical-inline" mode. As expected, the EM data are somewhat simpler than those of magnetic data due to their dipolar nature.

Unexploded Ordnance at Jefferson Proving Ground

As the last example, we present a set of magnetic and EM data obtained over a 200-ft by 200-ft plot in Jefferson Proving Ground (JPG), Indiana, where unexploded ordnance items presumably are buried. Like the INEL site, the Army Environmental Center established the JPG site to test various ground and airborne geophysical methods for detecting buried unexploded ordnance (UXO). We chose to include this example because the targets are small, isolated objects that should ideally represent the characteristics of a point source. Therefore, we expect that the comparison between magnetic and EM data should be relatively simple.

Magnetic data were collected using a Geometrics G858

Table 1. Waste forms placed in the INEL Cold Test Pit Calibration Cell.

Item	*Waste form type*	*Dimensions*	*Weight (kg)*	*Contents*
A	Drum with liner (55 gal)	24 in. dia x 36 in.	380	Concrete
B	Plastic drum (30 gal)	18 in. dia x 29 in.	105	Salt water
C	Drum with liner (55 gal)	24 in. dia x 36 in.	1.5	Foam
D	Wood box	2 x 4 x 4 ft	54	Wood and paper
E1	Wood box	2 x 4 x 4 ft	44	Wood and paper
E2	Wood box	2 x 4 x 4 ft	411	Ferrous metals
F	Wood box	2 x 4 x 4 ft	252	Mixed metals
G	Wood box	2 x 4 x 4 ft	405	Nonferrous metals
H	Wood box	2 x 4 x 4 ft	911	Dense-pack metals
File 1	5-drawer metal file cabinet	14 x 28 x 57 in.	25	Empty
File 2	5-drawer metal file cabinet	14 x 28 x 57 in.	25	Empty

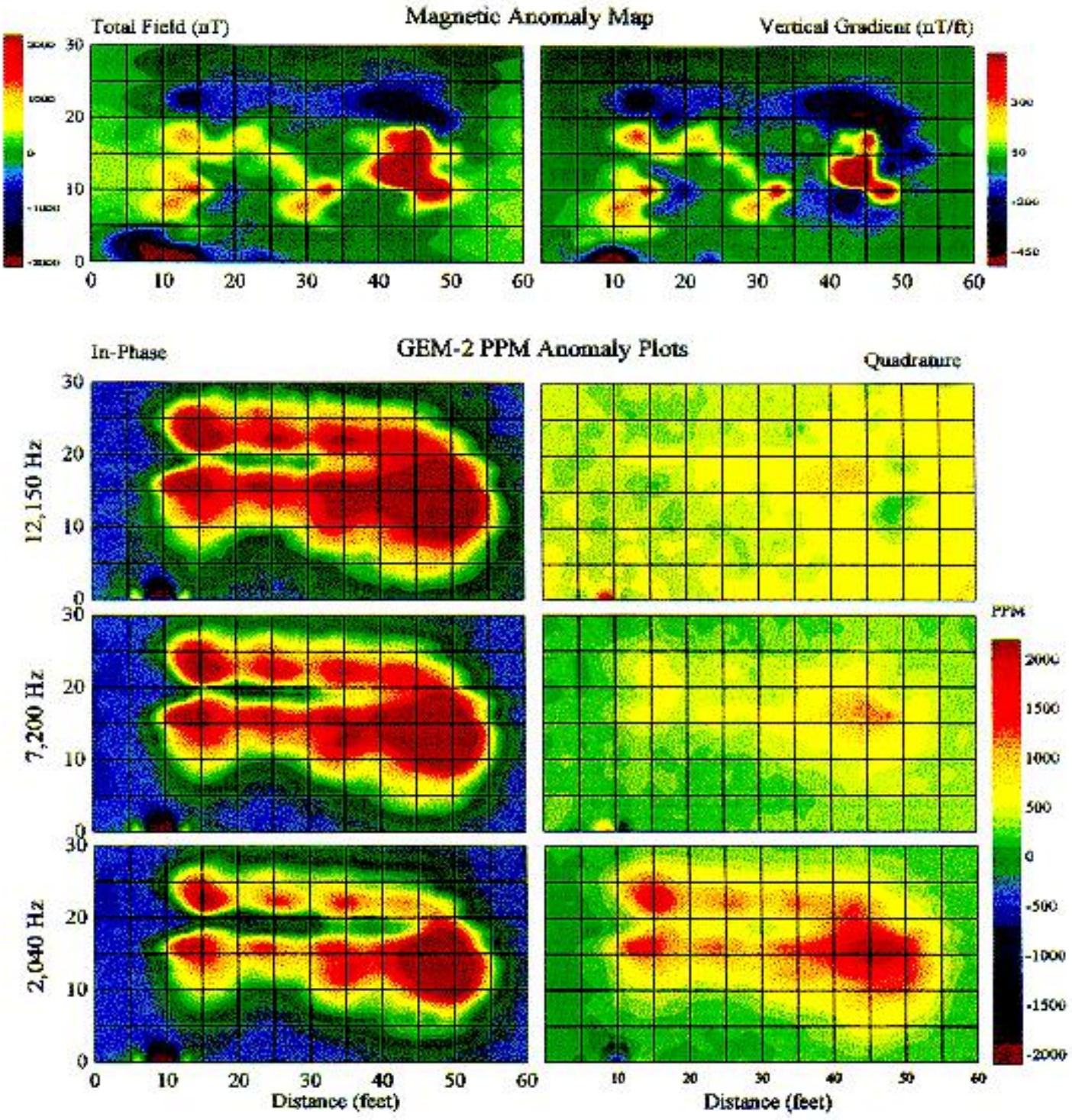

Figure 12. The total field and vertical magnetic gradient maps (top) and the GEM-2 data at three frequencies over the Calibration Cells, INEL.

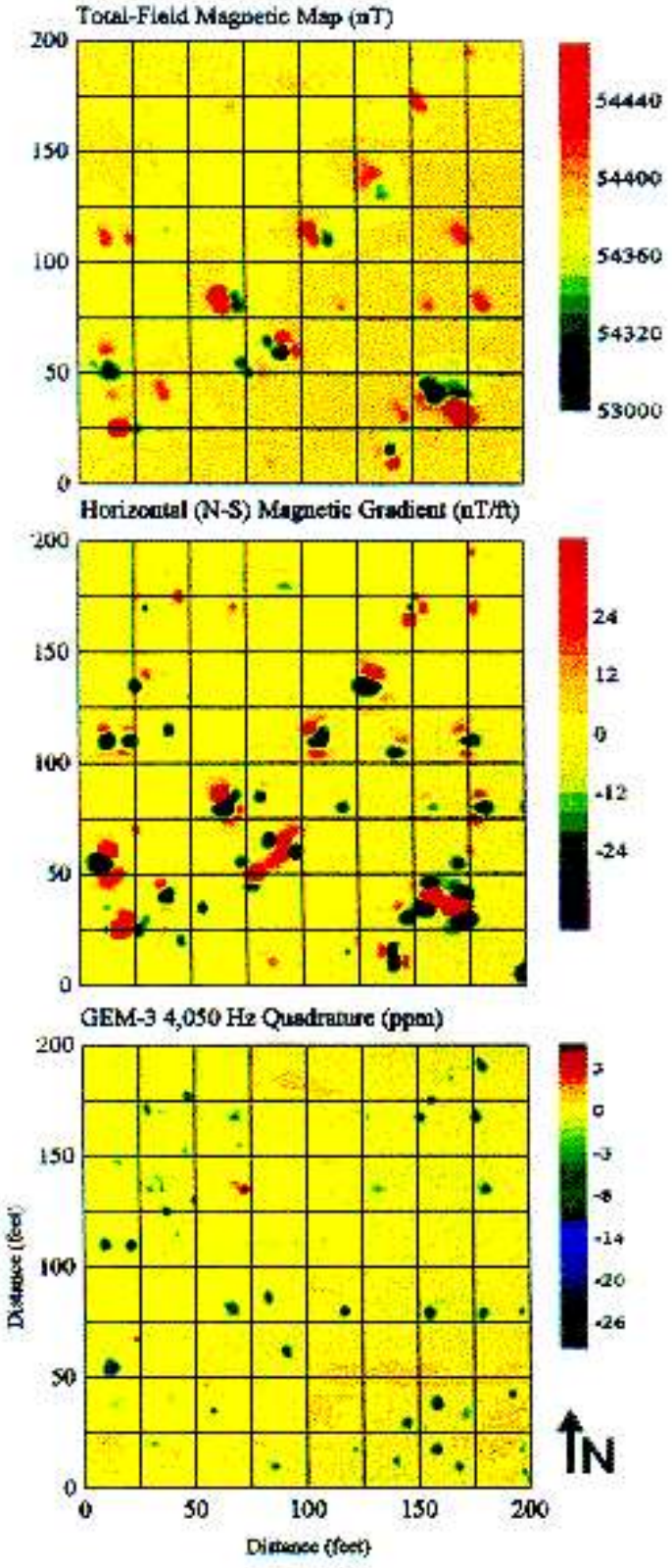

Figure 13.The total-field (top), the north-south, horizontal magnetic gradient (middle), and the GEM-3 4,050 Hz quadrature at a 200-ft by 200-ft plot in Jefferson Proving Ground, Indiana. The targets are buried unexploded ordnance.

cesium-vapor magnetometer with two sensors. Figure 13 shows the total field map (top) at about one foot above the ground as well as the north-south, horizontal magnetic gradient (middle). The EM data were collected at this site using the GEM-3, a monostatic broadband EM induction sensor (Won et al., 1997). We show in fig. 3 (bottom) the GEM-3 data only at 4,050 Hz in quadrature.

It is evident from the total field magnetic data that most UXOs can be represented by a single dipole source with varying moments and orientations. Dipole orientations in fig. 13 are almost random with respect to the magnetic north at this location, implying that the buried objects may have significant permanent magnetic moments. The UXO are likely located at the steepest slope connecting local positive and negative anomalies.

When we measure the horizontal gradient (in the north-south direction in this case), an object appears to be having a higher pole source (e.g., a spatial derivative of a dipole is a quadruple) as indicated in fig. 13 (middle). One advantage of the horizontal magnetic gradient is that the object is now located at the central peak (or valley) anomaly straddling two valleys (or peaks); this central anomaly location, again, renders the data interpretation more intrinsic than does the total-field data.

The GEM-3 anomaly map is shown in fig. 13 (bottom). Almost all targets now appear to be monopolar anomalies, which makes the target positioning very simple. For a couple of targets in fig. 13, the GEM-3 anomaly appears to be in an opposite color (red vs. blue) indicating phase rotations, which we found occur commonly depending on the target metal types (ferrous or non-ferrous). Because of this phase rotation, a target may be detected only within certain frequency windows, further supporting the need for multifrequency measurements.

Conclusions

Magnetic and EM methods are perhaps the most convenient and popular geophysical survey methods due to non-intrusiveness, light field logistics, and high survey speed. One should always consider the two methods as the precursor to any geophysical surveys. Often, the data resulting from the two methods are sufficient for characterizing shallow buried objects.

Owing to its monopolar nature, the EM data, particularly those from monostatic or almost monostatic sensors, are superior in locating a buried object to magnetic data. Additional advantages of the EM method come from the fact that it senses both electrically conductive and magnetically permeable targets. In contrast, the magnetic method responds only to permeable, or ferrous, metals. In that sense, the magnetic method may be considered a subset of the EM method, or it is a special "passive" EM method at zero frequency. Broadband EM measurements may lead us not only to an improved method of detection, but also to a possible discrimination capabilities

in terms of target's material composition.

Acknowledgements

The GEM-2 survey at the Cloud Chamber, Nevada Test Site, was funded by Los Alamos National Laboratory through Dr. Allen Cogbill. The survey over the Anacostia Metro tunnels in Washington, D.C. was funded by Oak Ridge National Laboratory through Dr. Steve Norton. The data from the Jefferson Proving Ground, Indiana, was obtained under a contract with PRC Environmental Management, Inc. which was, in turn, funded by the U.S. Army Environmental Center (AEC), Aberdeen Proving Ground, Maryland.

References

Cogbill, A.H., 1995, Ground magnetic survey at the NTS Cloud Chamber, Los Alamos National Laboratory Report LAUR-95-1654, 9 p.

Wait, J.R., 1953, A conducting permeable sphere in the presence of a coil carrying and oscillating current, Canadian Jour. Physics, **31**, p. 670.

Won, I.J., Keiswetter, D.A., Fields, G. R. A., and Sutton, L. C., 1996, GEM-2: A new multifrequency electromagnetic sensor, Journal of Environmental and Engineering Geophysics, **1**, pp. 129 - 138.

Won, I.J., Keiswetter, D.A., Hanson, D. R., Novikova, E., and Hall, T. M., 1997, GEM-3: A monostatic broadband electromagnetic induction sensor, **2**, pp. 53 - 64.